X-751-71-513
PREPRINT

NASA TM X- 65905

PERFORMANCE OF CONVOLUTION CODING CONCATENATED WITH MFSK MODULATION IN A GAUSSIAN CHANNEL

A. K. CHOUDHURY

(NASA-TM-X-65905) PERFORMANCE OF CONVOLUTION CODING CONCATENATED WITH MFSK MODULATION IN A GAUSSIAN CHANNEL A.K. Choudhury (NASA) Dec. 1971 32 p CSCL 17B

N72-25190

Unclas
G3/07 30235

DECEMBER 1971

RECEIVED JUN 1972 NASA STI FACILITY INPUT BRANCH

GSFC — GODDARD SPACE FLIGHT CENTER
GREENBELT, MARYLAND

Reproduced by
NATIONAL TECHNICAL
INFORMATION SERVICE
U S Department of Commerce
Springfield VA 22151

PERFORMANCE OF CONVOLUTION CODING CONCATENATED WITH MFSK MODULATION IN A GAUSSIAN CHANNEL

A. K. Choudhury

December 1971

Goddard Space Flight Center
Greenbelt, Maryland

CONTENTS

PERFORMANCE OF CONVOLUTION CODING CONCATENATED WITH MFSK MODULATION IN A GAUSSIAN CHANNEL

1. Introduction

In a m-ary frequency-shift-keyed communication link (MFSK) one of the M messages, x_ℓ; ($\ell = 1, 2, 3, \ldots M$) is transmitted during each T second interval as a sinusoidal tone at frequency f_ℓ. This tone is then modulated onto a carrier frequency f_c to produce the single transmitted frequency $f_c + f_\ell$. Ideally, at the receiver the carrier frequency f_c is removed and the resulting signal frequency f_ℓ is detected using a spectral analysis receiver. In order to reduce the probability of a bit error and to increase the available bit rate for the same system parameters (error rate, transmitter power, range etc.) concatenation of convolution coding with coded MFSK communication link has been proposed. In this report we shall study the improvement in db due to concatenation over the conventional m-ary coding. The performance of convolution coded system depends on the channel parameters R_{comp} [1] and $E_0(\rho)$ [2]. For a discrete memory less channel with M inputs and J outputs,

$$E_0(\rho) = \max_{\{p_j\}} \left[-\log_2 \sum_{j=1}^{J} \sum_{k=1}^{M} p_k \, q_{jk}^{1/1+\rho} \right]^{1+\rho} \tag{1}$$

where $\{p_j\}$ are the a priori input probabilities, and

$$R_{comp} = E_0(1). \tag{2}$$

It can be shown by random coding arguments that the undetected error probability using Fano decoding algorithm satisfies the following bounds:

$$P_E \leq \begin{cases} A2^{-K R_{comp}/R_N}; & \text{for } R_N \leq R_{comp} \\ A2^{-K\rho}; & \text{for } R_N > R_{comp} \end{cases}$$

where A is a constant in the order of unity.

K is the code constraint length. R_N is the code rate in bits per transmitted waveform. ρ is the pareto exponent. The pareto exponent ρ is the solution of the equation

$$\frac{E_0(\rho)}{\rho} = R_N \tag{3}$$

The decoder computational distribution must be known to determine the necessary buffer size. If c is a random variable equal to the number of decoder computations required to decode an information bit, then c has a pareto distribution, i.e.,

$$\text{Prob}\,(c > L) = BL^{-\rho} \tag{4}$$

where B is a constant in the order of unity. It follows from eq. (4) that ρ must be greater than 1 for finite average computation. Therefore $E_0(1) = R_{comp}$ is called the computational cut off rate.

A space communication channel can be accurately modelled on an additive Gaussian noise channel. Digital data is transmitted over this channel by coding it into a set of analog waveforms suitable for transmission over the channel. A demodulator converts the received signal back into digital form. From the point

of view of the encoder and decoder the channel consists of the combination of the modulator, white Gaussian noise channel, and demodulator. The relative efficiency of various modulation and demodulation schemes can be compared by calculating E_b/N_0 necessary for $R_{comp} = R_N$, where E_b is the signal energy per information bit and N_0 is the one-sided noise spectral density. In this report the results of calculations for orthogonal modulation with non-coherent detection and Q-level correlator quantization are presented.

2. Channel Model

It will be assumed that the signal transmitted is one of the M equal energy, orthogonal signals

$$s_j(t) = e_j(t) \sin \omega_0 t, \quad j = 1, 2, \ldots M \tag{5}$$

and

$$\int_0^T s_j(t)\, s_i(t)\, dt = E_N \delta_{ji}, \quad \delta_{ji} = 1, \; y_j = i \qquad = 0, \; y_j \neq i \tag{6}$$

The received signal is

$$y(t) = e_j(t) \sin(\omega_0 t + \theta) + n(t) \tag{7}$$

where θ is a random variable uniformly distributed over $(0, 2\pi)$, $n(t)$ is white Gaussian noise with spectral density $N_0/2$.

The maximum likelihood receiver for this non-coherent channel calculates the M quantities

$$y_i = \sqrt{x_i^2 + \omega_i^2}, \text{ for } i = 1, 2, \ldots M \tag{8}$$

where

$$x_i = \sqrt{\frac{2}{N_0 E_N}} \int_0^T y(t)\, e_i(t) \sin \omega_0(t)\, dt \tag{9}$$

$$\omega_i = \sqrt{\frac{2}{N_0 E_N}} \int_0^T y(t)\, e_i(t) \cos \omega_0(t)\, dt\,. \tag{10}$$

The device that performs these calculations is known as an envelope detector. The correlator outputs are statistically independent and have probability densities

$$f(y_i/s_i) = y_i\, e^{-\frac{(y_i^2 + a^2)}{2}}\, I_0(ay_i)\, u(y_i)$$

$$= f_{s+n}(y_i), \quad j = i \tag{11}$$

$$f(y_i/s_i) = y_j\, e^{-\frac{y_j^2}{2}}\, u(y_j)$$

$$= f_n(y_j), \text{ for } j \neq i \tag{12}$$

where

$$a = \sqrt{\frac{2E_N}{N_0}}\,, \quad u(\cdot) \text{ is the unit step function.}$$

In this study the correlator outputs are quantized to one of the Q levels. The receiver output is a vector consisting of a list of the M correlator quantum levels. Therefore the channel has Q^M possible outputs and M possible inputs. With this method the optimum output can be approached by increasing fine quantization.

3. R_{comp} for Unquantized Outputs

R_{comp} for the exact optimum correlator output case can be found by letting the quantization become infinitely fine. From eqs. (1) and (2) it follows that

$$R_{comp} = \max_{\{p_i\}} \left\{ -\log_2 \int_{\infty}^{\infty} \left[\sum_{i=1}^{M} p_i \sqrt{f(Y|s_i)} \right]^2 dY \right\} \qquad (13)$$

where Y is the correlator output vector and $f(Y|s_i)$ is the joint density for the correlator outputs given input s_i. For symmetric channels R_{comp} is a maximum for equally likely inputs, i.e., $p_i = 1/M$ for all i. On substituting eqs. (11)-(12) in eq. (13) it follows that

$$R_{comp} = \log_2 \frac{M}{1 + (M-1)\, e^{-u^2/2} \left[\int_0^{\infty} x\, e^{-x^2/2}\, I_0^{1/2}(ax)\, dx \right]^2} .$$

R_{comp} vs E_N/N_0 for M = 2, 4, 8, 16, 32, 64 is plotted in the enclosed figures.

4. R_{comp} with Q-Level Quantization

To approximate the exact output case the half line $(0, \infty)$ can be divided into a disjoint set of intervals Δj such that $U_j \Delta_j = (0, \infty)$. If the correlator output $y_\ell \in \Delta_j$, then the quantized value is taken to be $\hat{y}_\ell = j$. Let

$$P(\hat{y}_j = i/s_\ell) = \int_{\Delta_i} f_{s+n}(x)\, dx = P_{s+n}(i)$$

for $\ell = j$

$$= \int_{\Delta_i} f_n(x)\, dx = P_n(i)$$

for $\ell \neq j$

From eqs. (1) and (2) it follows that

$$R_{comp} = \log_2 \frac{M}{1 + (M-1)\left[\sum_{i=1}^{Q} \sqrt{P_{s+n}(i)\, P_n(i)}\right]^2} \tag{14}$$

For simplicity equal width quantization intervals were chosen. The quantizer input-output relationship is illustrated below. Optimum thresholds were searched for by trial and error. The optimum thresholds depends on the signal-to-noise ratio. Therefore, sub optimum thresholds good for a wide range of signal-to-noise ratios (0-19) were chosen and shown in Table 1. R_{comp} vs E_N/N_0 for these thresholds are plotted.

Q \ T	T_1	T_2	T_3
2	3.0		
3	2.0	4.0	
4	1.5	3.0	4.5

Quantizer Thresholds

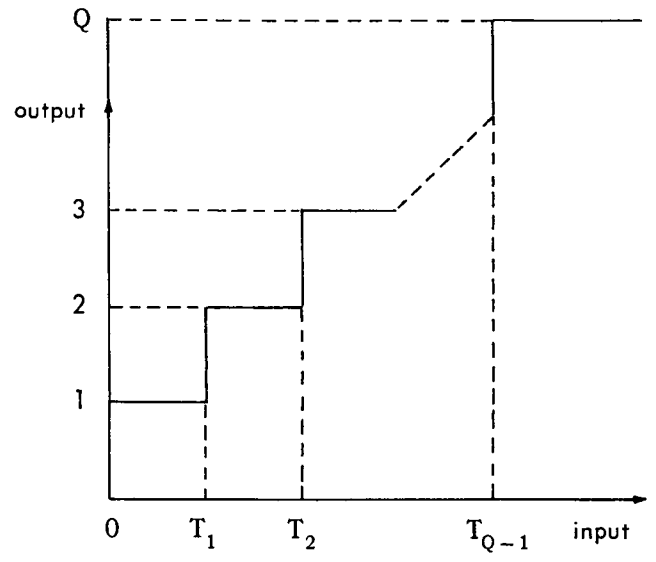

5. $E_0(\rho)$ vs ρ with Q-level Quantization.

For symmetric channels equally likely inputs, i.e., $p_i = 1/M$ for all i, maximize the expression for $E_0(\rho)$. Using the fact that the correlator outputs are statistically independent, equation (1) reduces to

$$E_0 = \log_2 \frac{M^{1+\rho}}{\left[\sum_{i} \cdots \sum_{y_m=1}^{Q} \sum_{\ell=1}^{M} \prod_{i=1}^{M} P(\hat{y}_\ell / k)^{1/1+\rho} \right]^{1+\rho}}$$

using the sub optimum thresholds of Table 1 calculated values of $E_0(\rho)$ vs ρ for various values of E_N/N_0 and M are plotted.

REFERENCES

1. J. M. Wozencraft and I. M. Jacobs, Principles of Communications Engineering, John Wiley & Sons, New York, 1965

2. R. G. Gallagar, "A Simple Derivation of the Coding Theorem and Some Applications." IEEE Transactions on Information Theory, January 1965, pp 3-18

3. I. M. Jacobs, "Sequential Decoding for Efficient Communication from Deep Space," IEEE Transactions on Communication Technology, Vol. com-15, No. 4, August 1967, pp 492-501

4. K. L. Jordan, "The Performance of Sequential Decoding in Conjunction with Efficient Modulation," IEEE Transactions on Communications Technology, Vol. com.-14, No. 3, June 1966, pp 283-297

5. R. Teoste, "M-ary Channel Quantization for Sequential Decoding," Lincoln Laboratory, M.I.T., JA 2817, June 28, 1966

6. M. C. Kim and S. A. Tretter, "Performance of Sequential Decoding with Biorthogonal Modulation and Q-Level Quantization," IEEE Transactions on Communications Technology, February 1971

7. H. D. Chadwick and J. C. Springett, "The Design of a Low Data Rate MFSK Communication System," IEEE Transactions on Communications Technology, December 1970

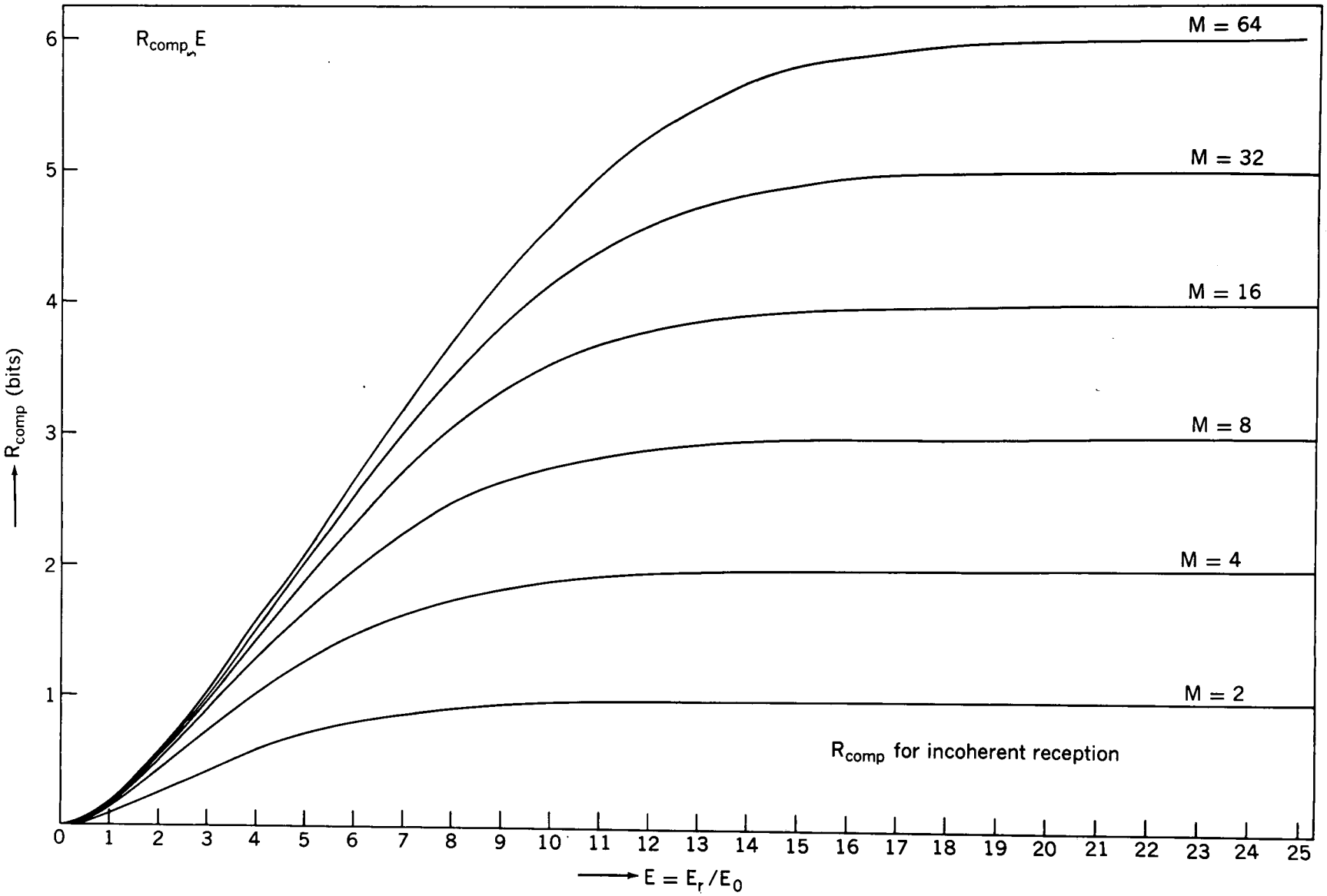
R_{comp} E
M = 64
M = 32
M = 16
M = 8
M = 4
M = 2
R_{comp} for incoherent reception
R_{comp} (bits)
$E = E_r / E_0$
0 1 2 3 4 5 6 7 8 9 10 11 12 13 14 15 16 17 18 19 20 21 22 23 24 25
1 2 3 4 5 6

FIGURE 1

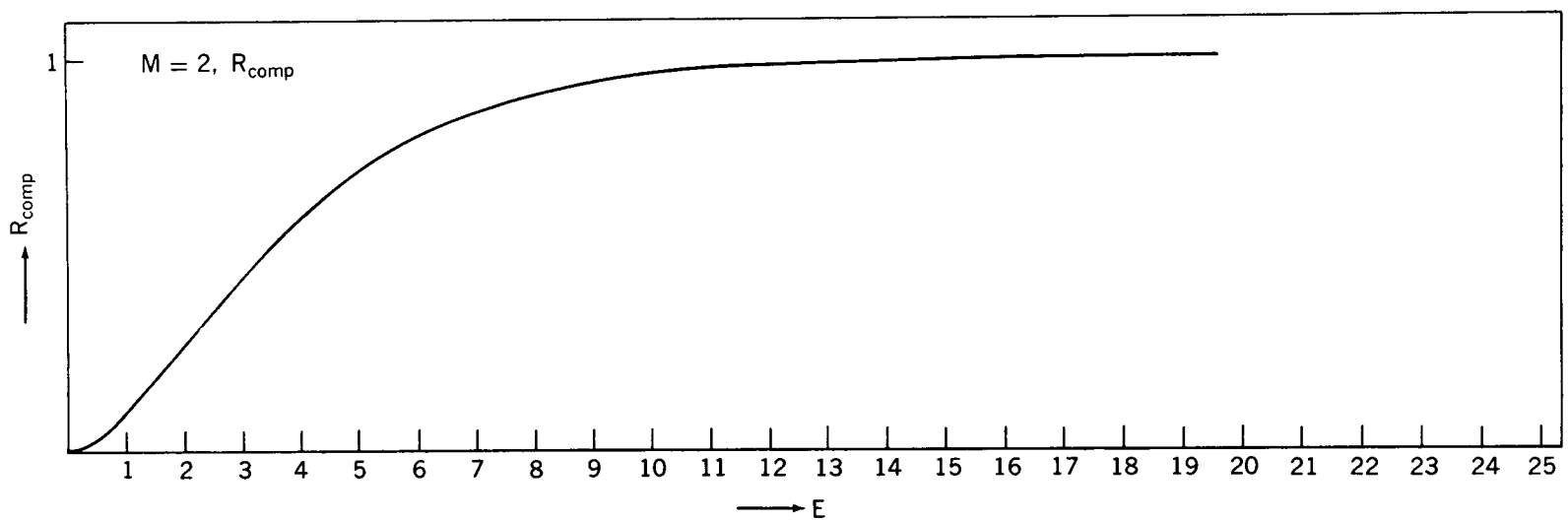
1
M = 2, R_{comp}
R_{comp}
1 2 3 4 5 6 7 8 9 10 11 12 13 14 15 16 17 18 19 20 21 22 23 24 25
E

FIGURE 2

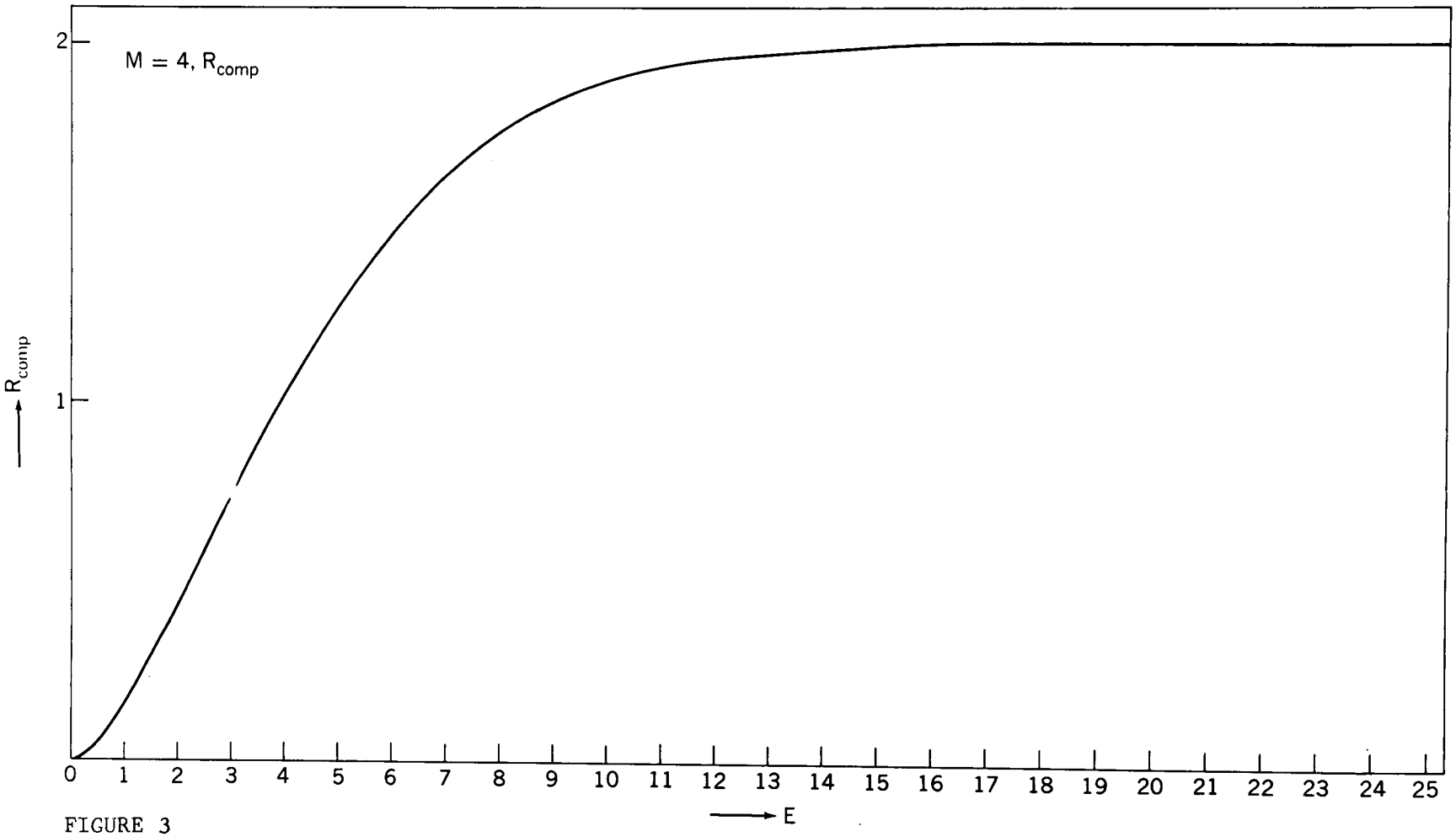
M = 4, R_{comp}
2
1
R_{comp}
0 1 2 3 4 5 6 7 8 9 10 11 12 13 14 15 16 17 18 19 20 21 22 23 24 25
E

FIGURE 3

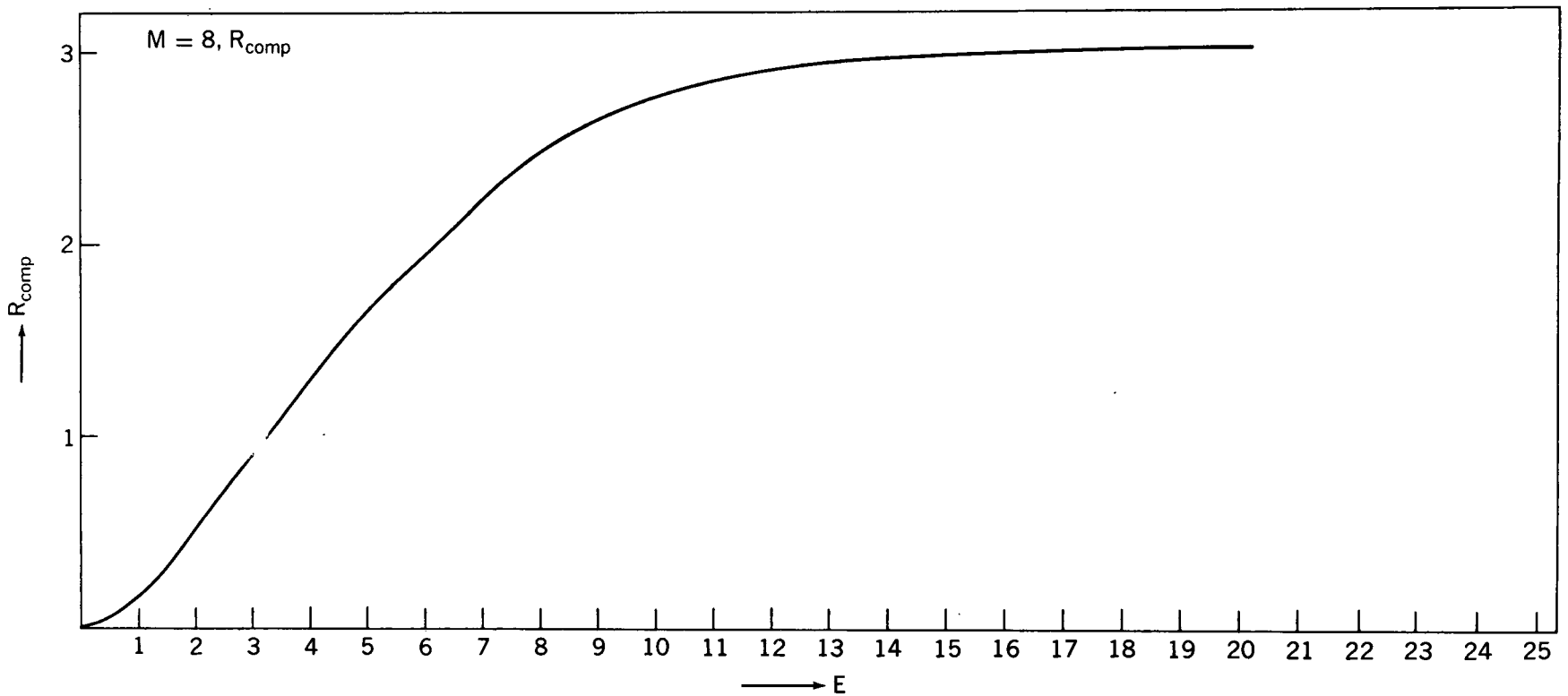
M = 8, R_{comp}
3
2
1
R_{comp}
1 2 3 4 5 6 7 8 9 10 11 12 13 14 15 16 17 18 19 20 21 22 23 24 25
E

FIGURE 4

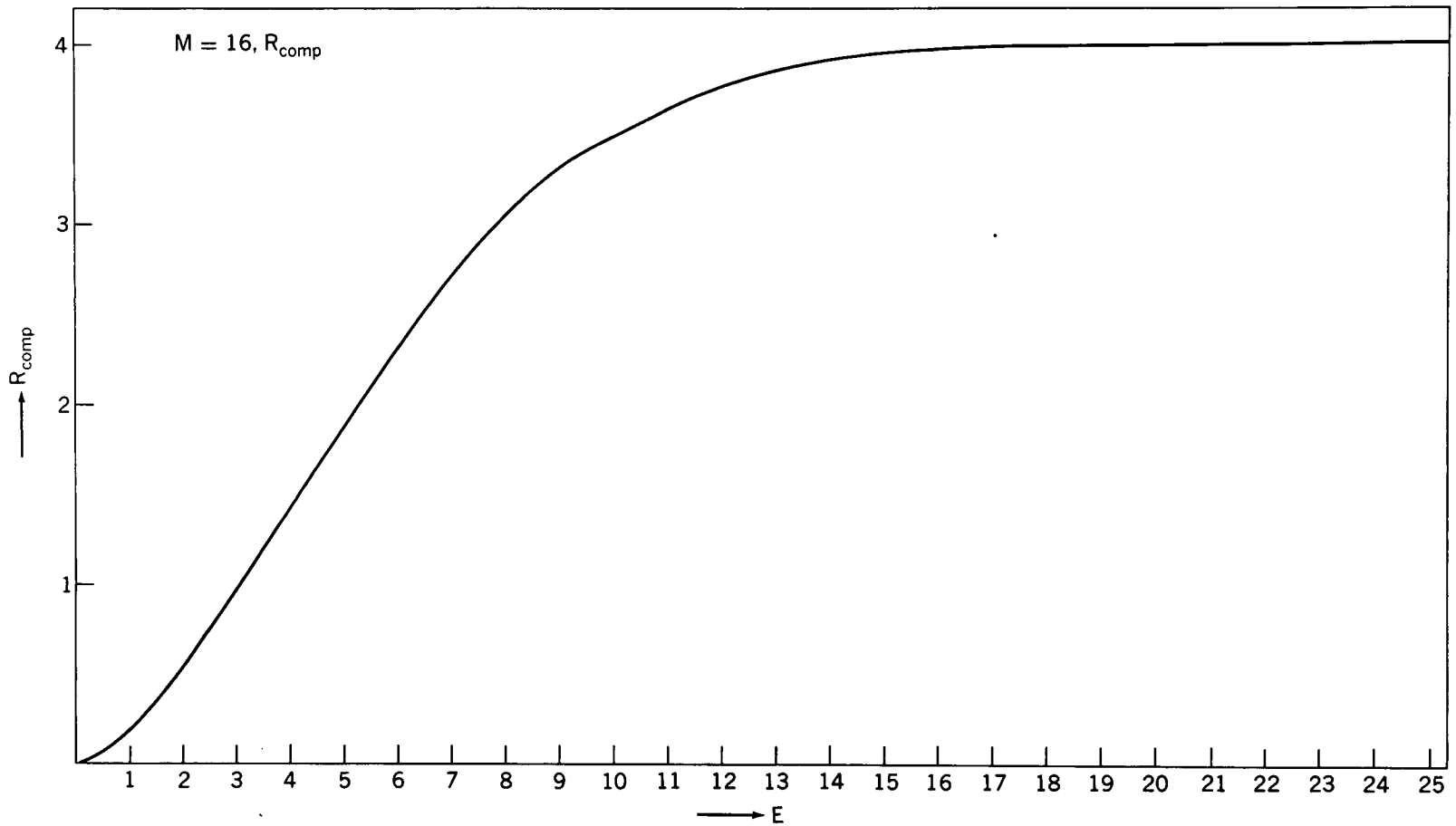
M = 16, R_{comp}
R_{comp}
4
3
2
1
1 2 3 4 5 6 7 8 9 10 11 12 13 14 15 16 17 18 19 20 21 22 23 24 25
E

FIGURE 5

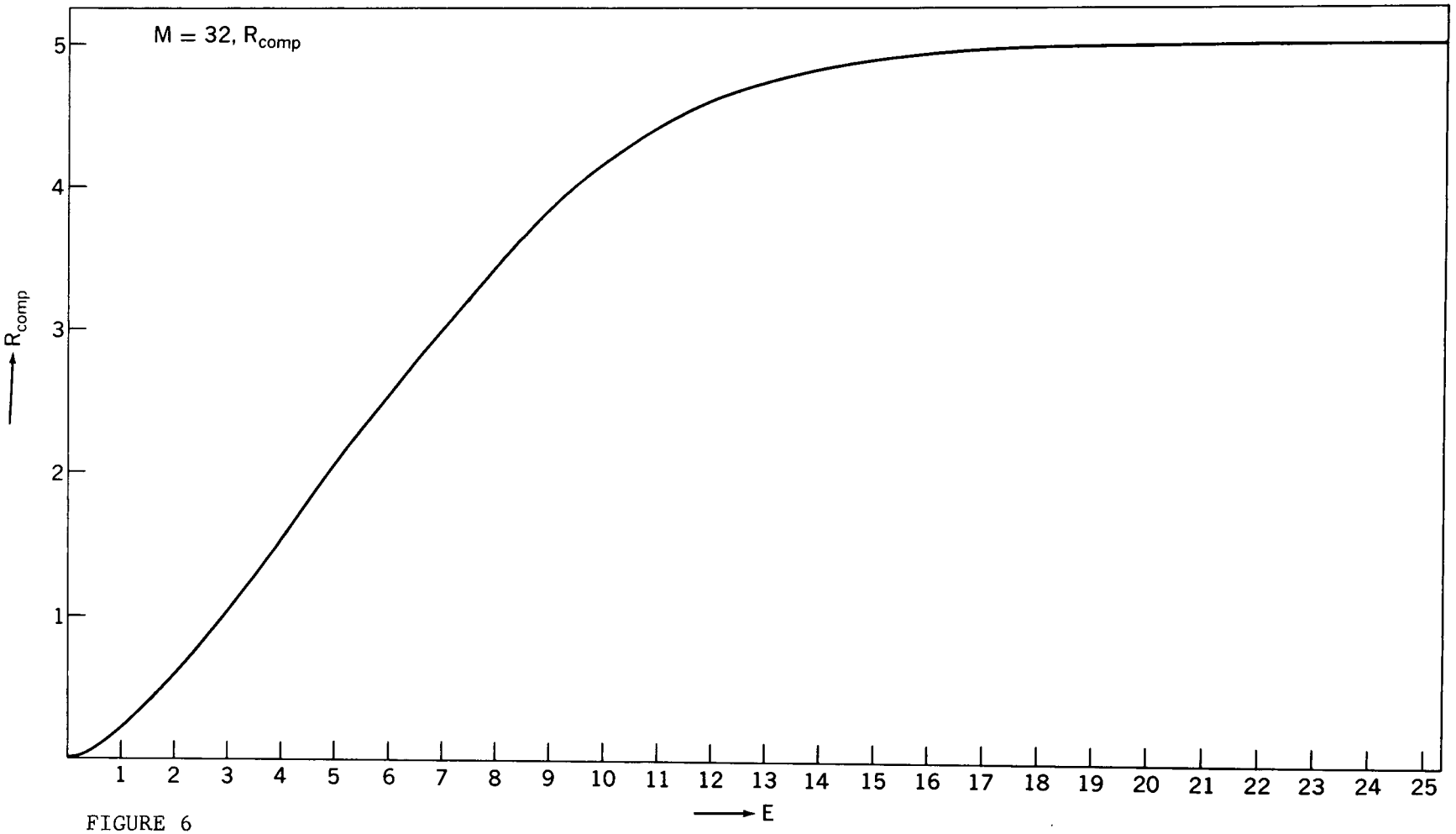
M = 32, R_{comp}
R_{comp}
5
4
3
2
1
1 2 3 4 5 6 7 8 9 10 11 12 13 14 15 16 17 18 19 20 21 22 23 24 25
E

FIGURE 6

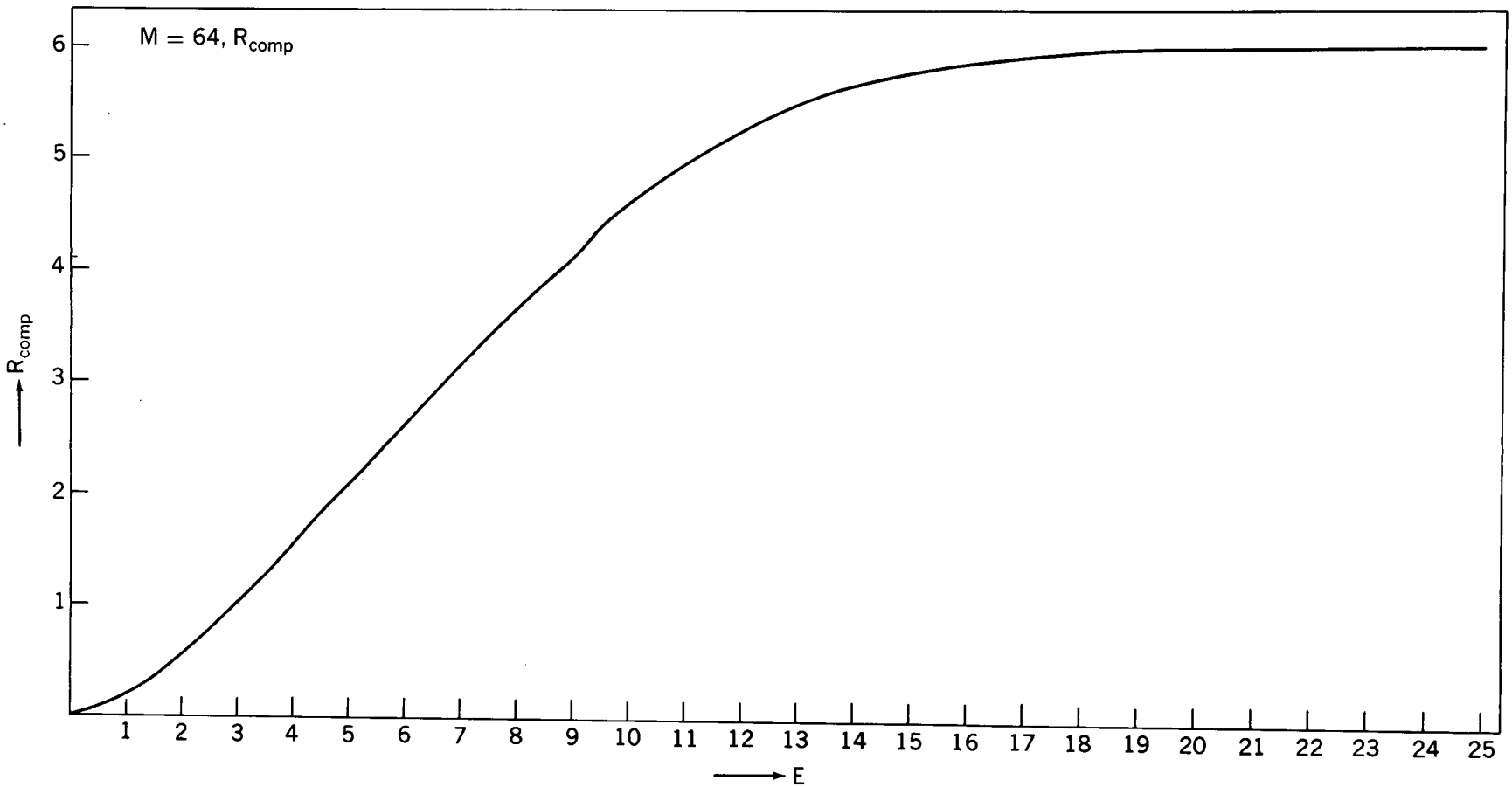
M = 64, R_{comp}
R_{comp}
6
5
4
3
2
1
1 2 3 4 5 6 7 8 9 10 11 12 13 14 15 16 17 18 19 20 21 22 23 24 25
E

FIGURE 7

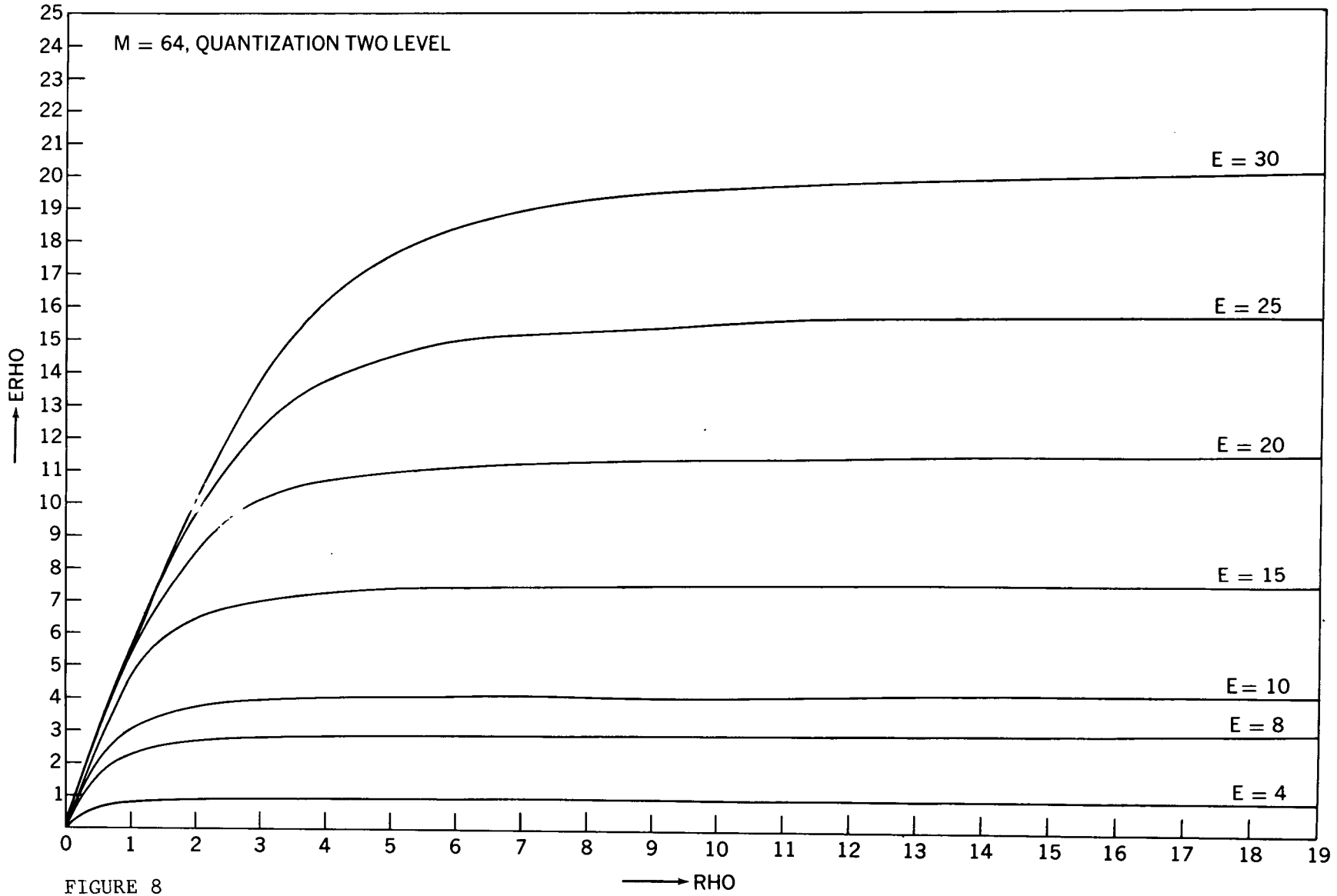
M = 64, QUANTIZATION TWO LEVEL
E = 30
E = 25
E = 20
E = 15
E= 10
E = 8
E = 4
ERHO
RHO
0 1 2 3 4 5 6 7 8 9 10 11 12 13 14 15 16 17 18 19
1 2 3 4 5 6 7 8 9 10 11 12 13 14 15 16 17 18 19 20 21 22 23 24 25

FIGURE 8

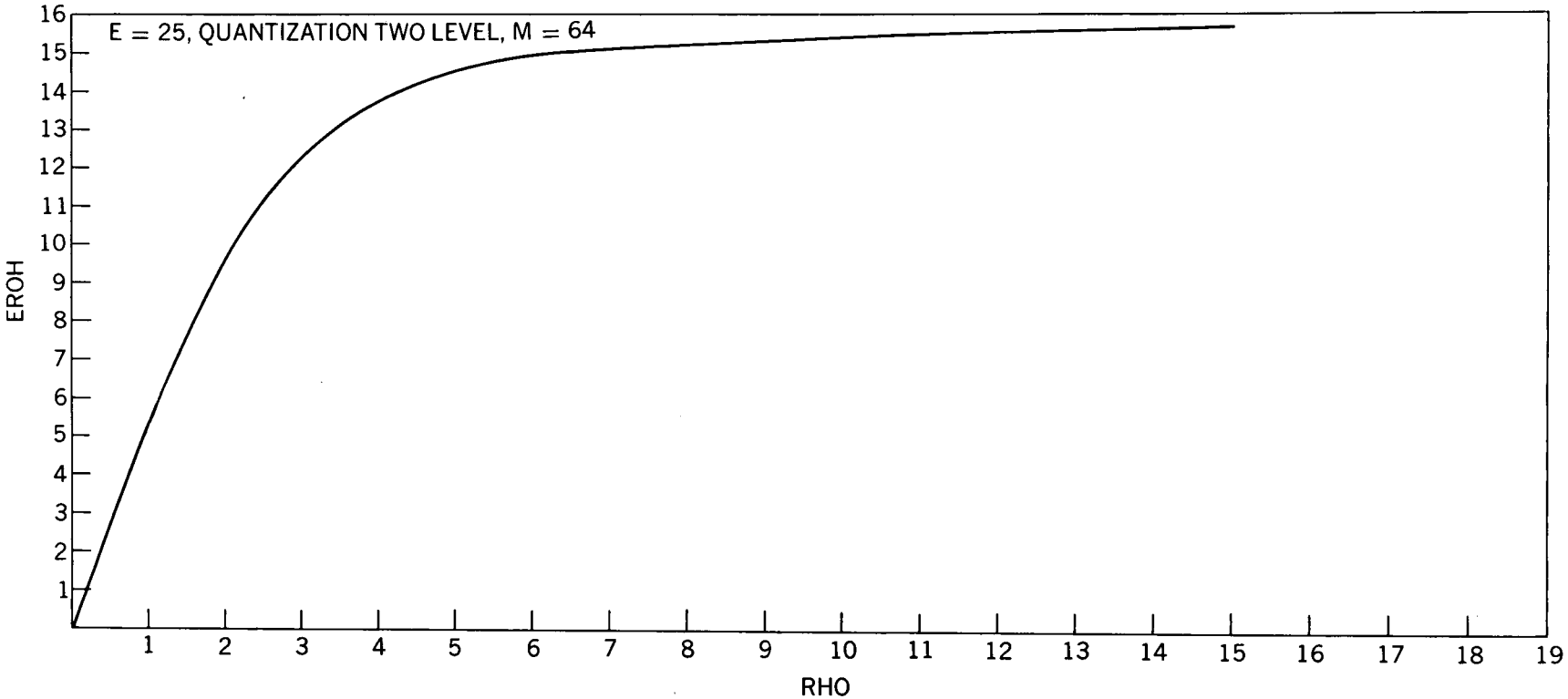
E = 25, QUANTIZATION TWO LEVEL, M = 64
EROH
RHO
16
15
14
13
12
11
10
9
8
7
6
5
4
3
2
1
1
2
3
4
5
6
7
8
9
10
11
12
13
14
15
16
17
18
19

FIGURE 9

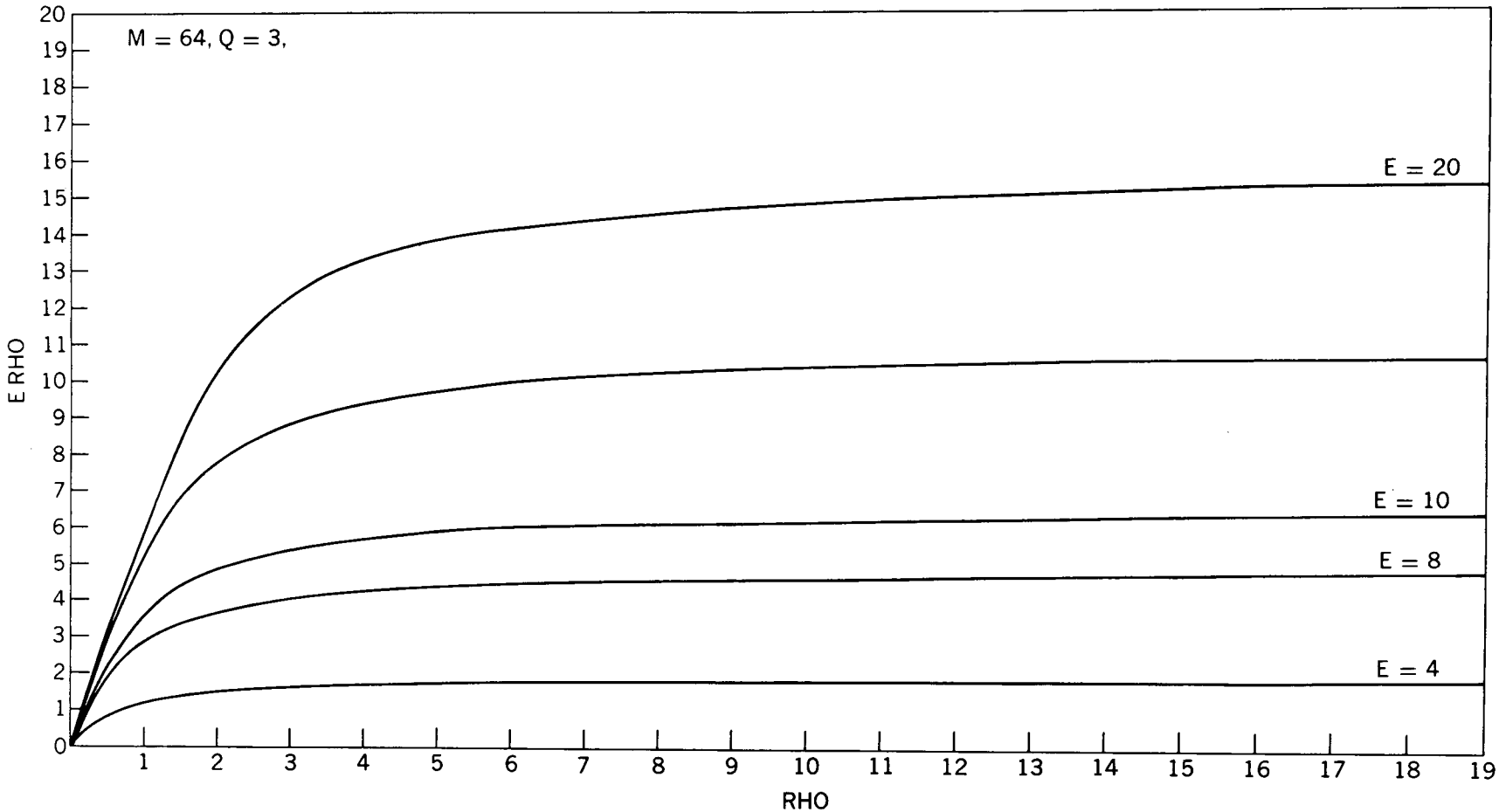
M = 64, Q = 3,
E = 20
E = 10
E = 8
E = 4
E RHO
RHO
0
1
2
3
4
5
6
7
8
9
10
11
12
13
14
15
16
17
18
19

FIGURE 10

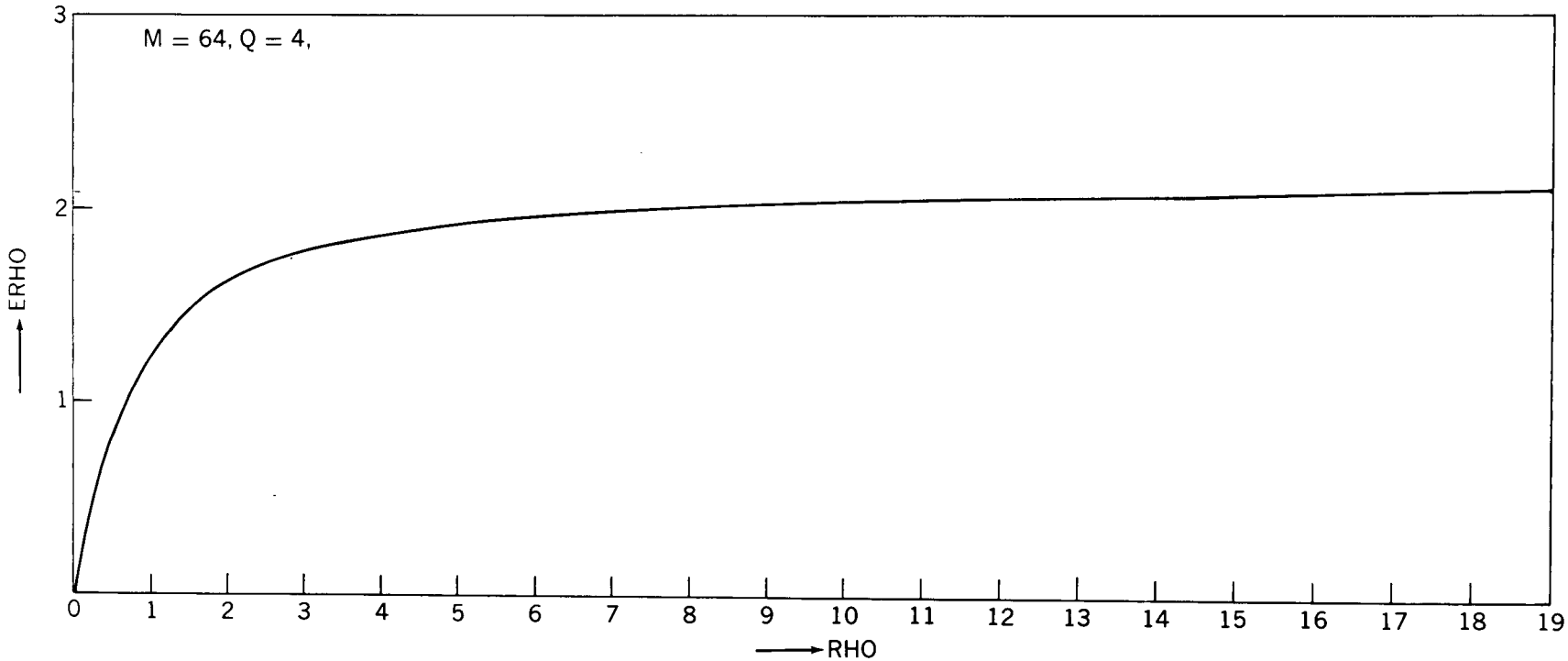

FIGURE 11

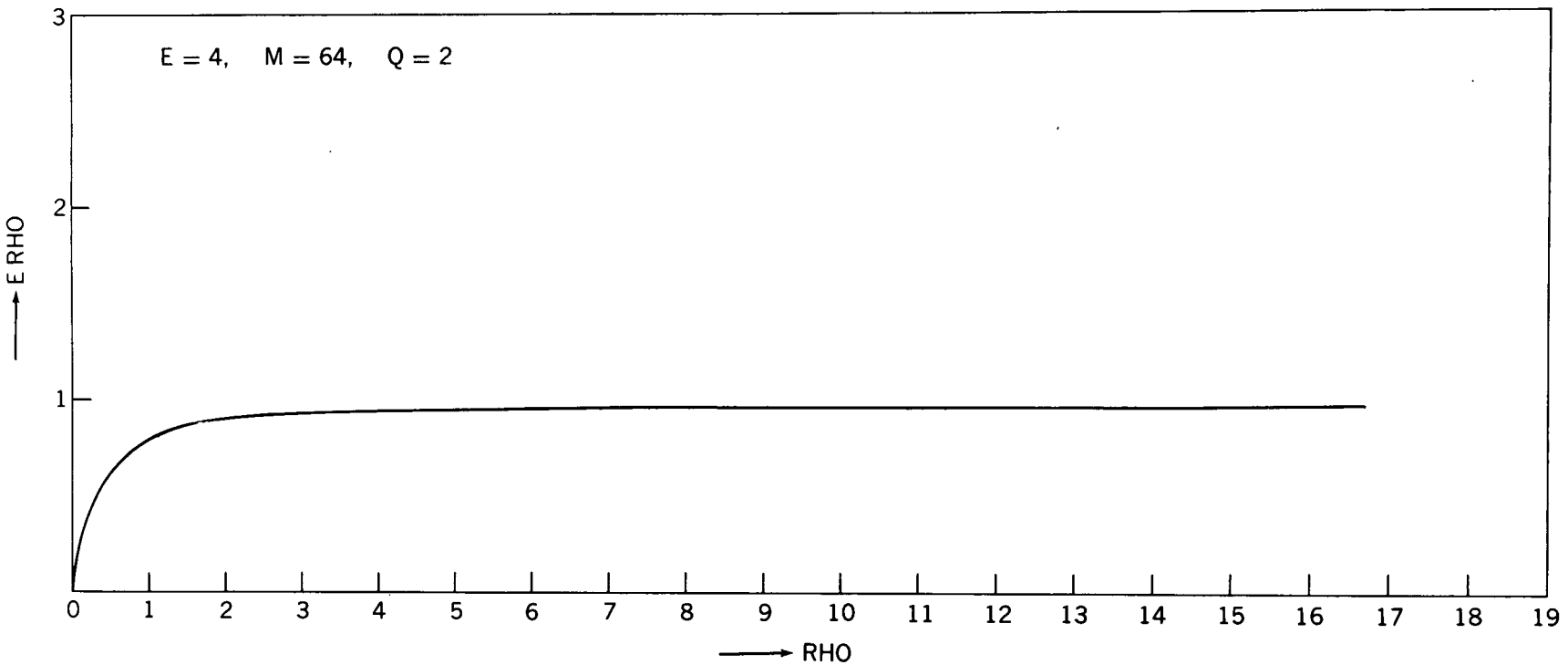

FIGURE 12

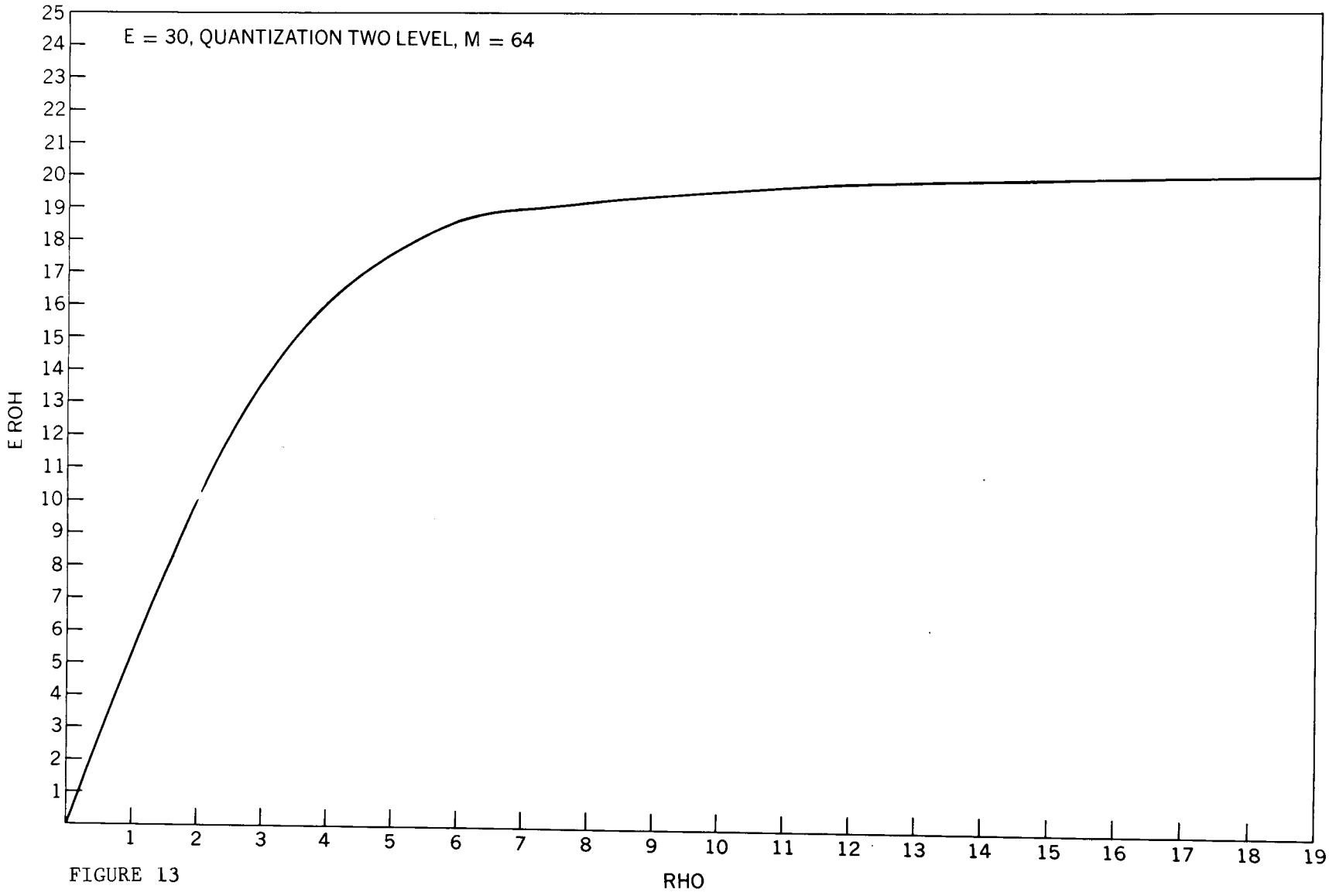
E = 30, QUANTIZATION TWO LEVEL, M = 64
E ROH
RHO
25
24
23
22
21
20
19
18
17
16
15
14
13
12
11
10
9
8
7
6
5
4
3
2
1
1 2 3 4 5 6 7 8 9 10 11 12 13 14 15 16 17 18 19

FIGURE 13

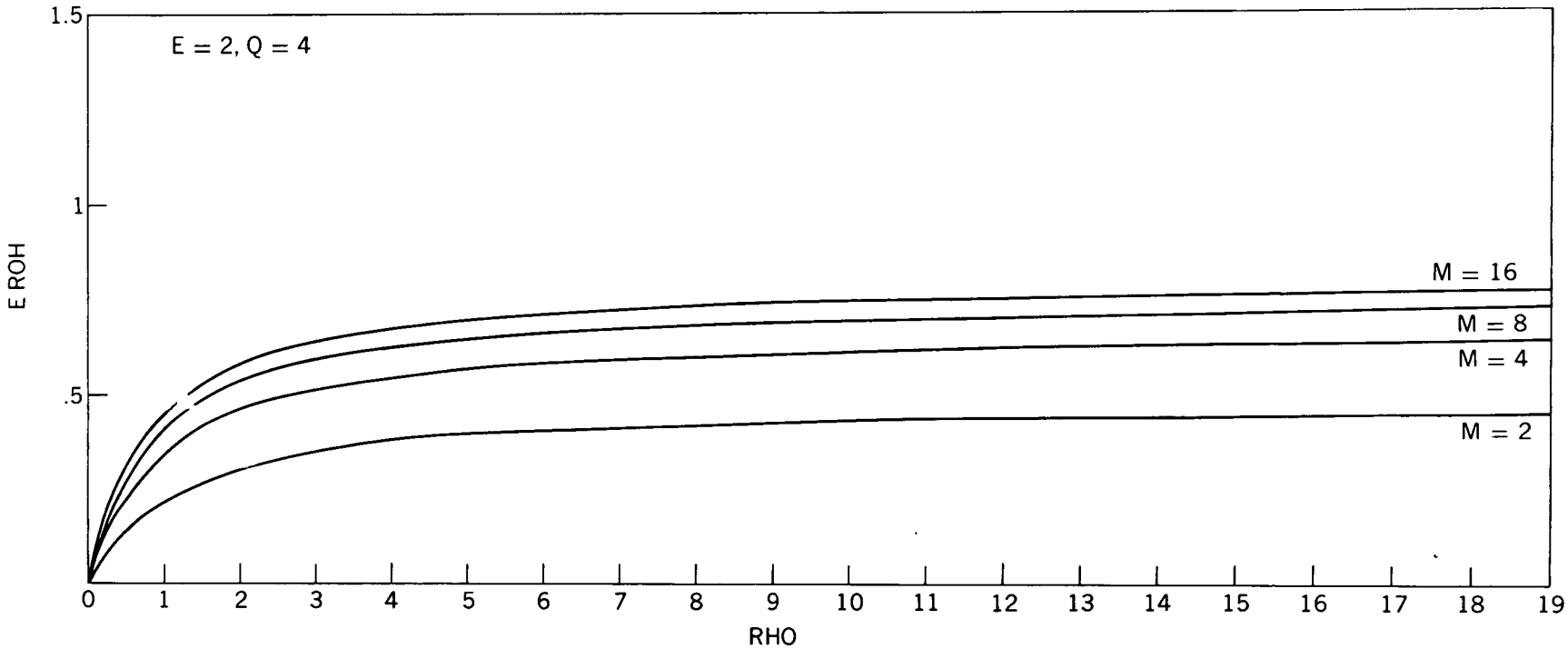
E = 2, Q = 4
E ROH
1.5
1
.5
M = 16
M = 8
M = 4
M = 2
0
1
2
3
4
5
6
7
8
9
10
11
12
13
14
15
16
17
18
19
RHO

FIGURE 14

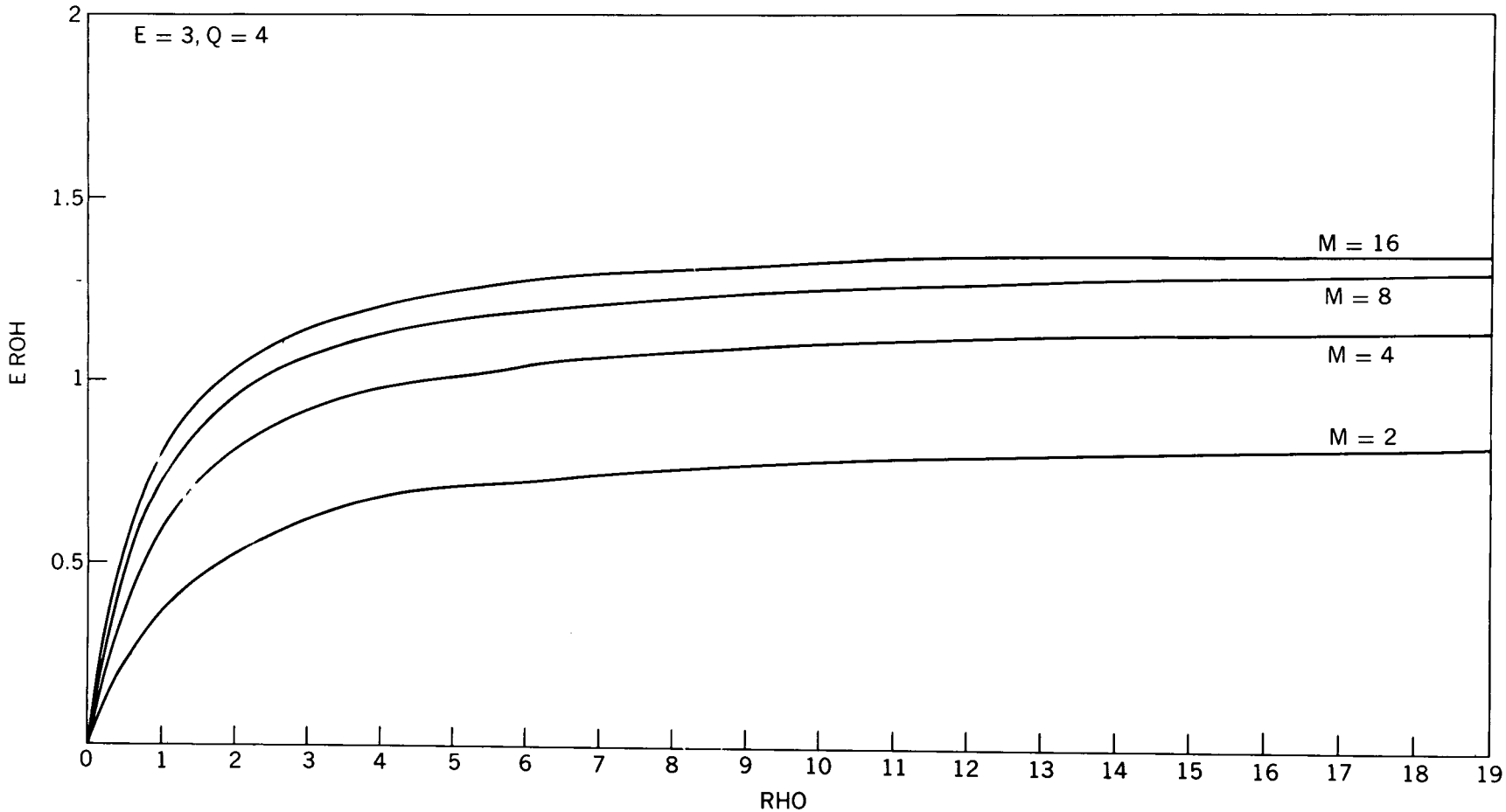
E = 3, Q = 4
M = 16
M = 8
M = 4
M = 2
E ROH
RHO
0
0.5
1
1.5
2
0 1 2 3 4 5 6 7 8 9 10 11 12 13 14 15 16 17 18 19

FIGURE 15

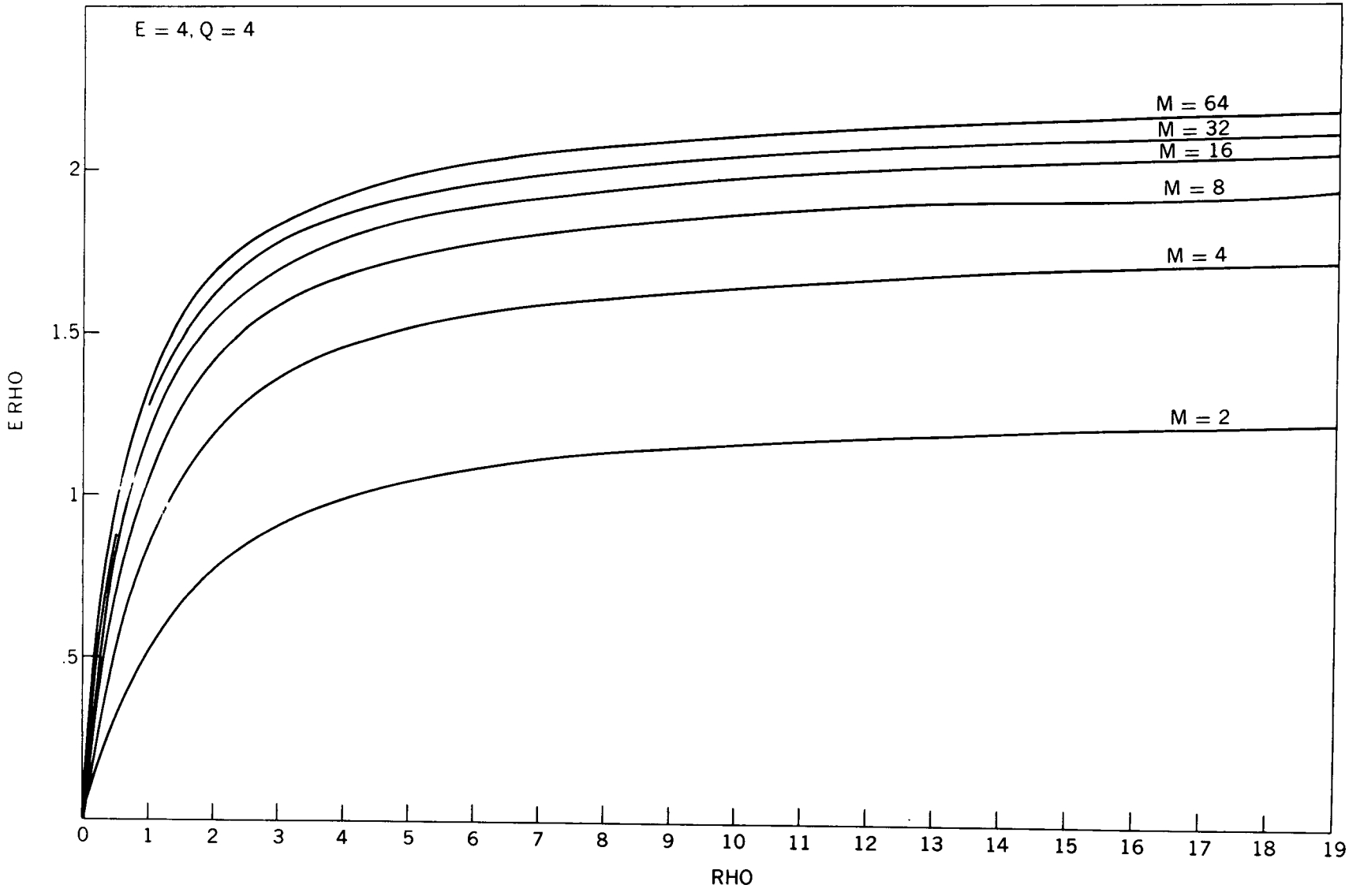
E = 4, Q = 4
M = 64
M = 32
M = 16
M = 8
M = 4
M = 2
E RHO
2
1.5
1
.5
0
1
2
3
4
5
6
7
8
9
10
11
12
13
14
15
16
17
18
19
RHO

FIGURE 16

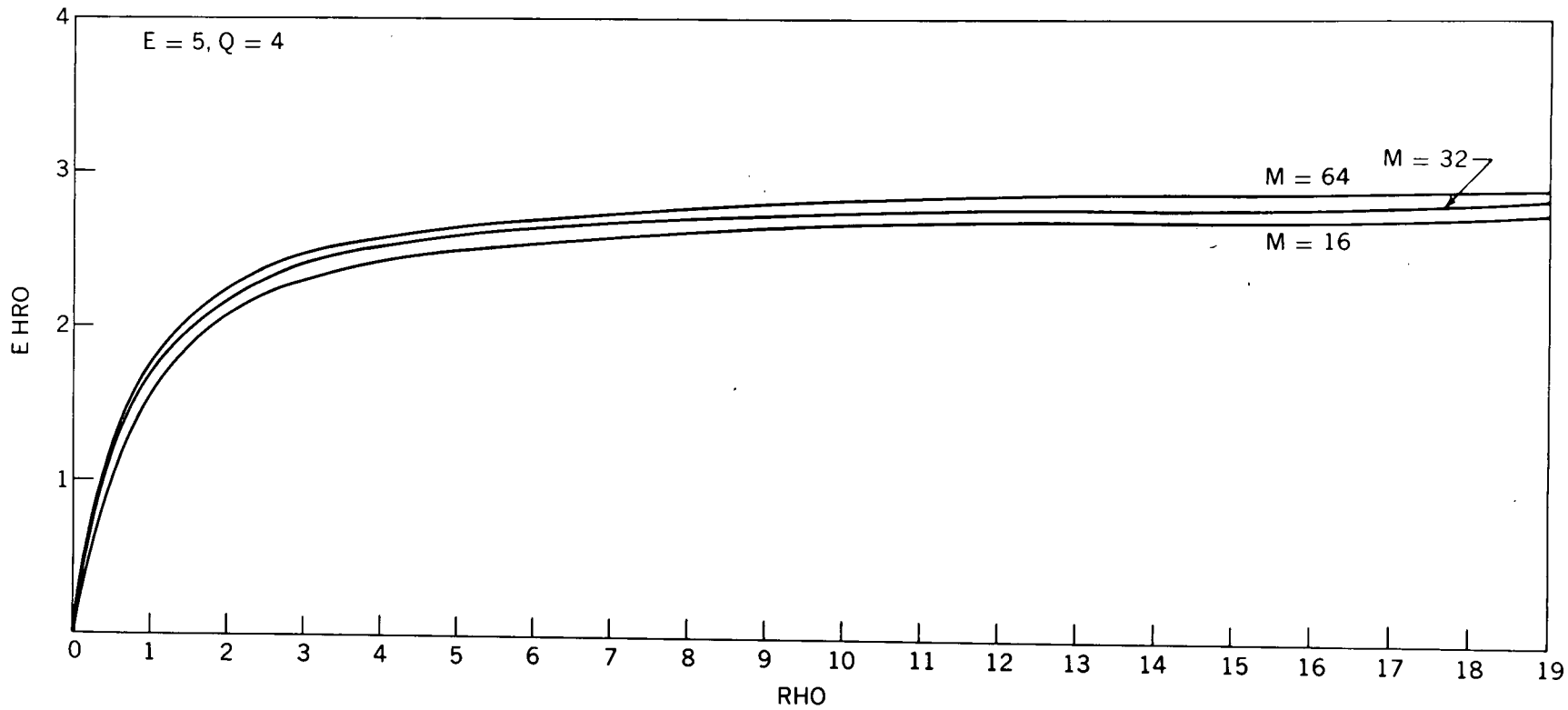
E = 5, Q = 4
M = 64
M = 32
M = 16
E HRO
RHO
0
1
2
3
4
5
6
7
8
9
10
11
12
13
14
15
16
17
18
19

FIGURE 17

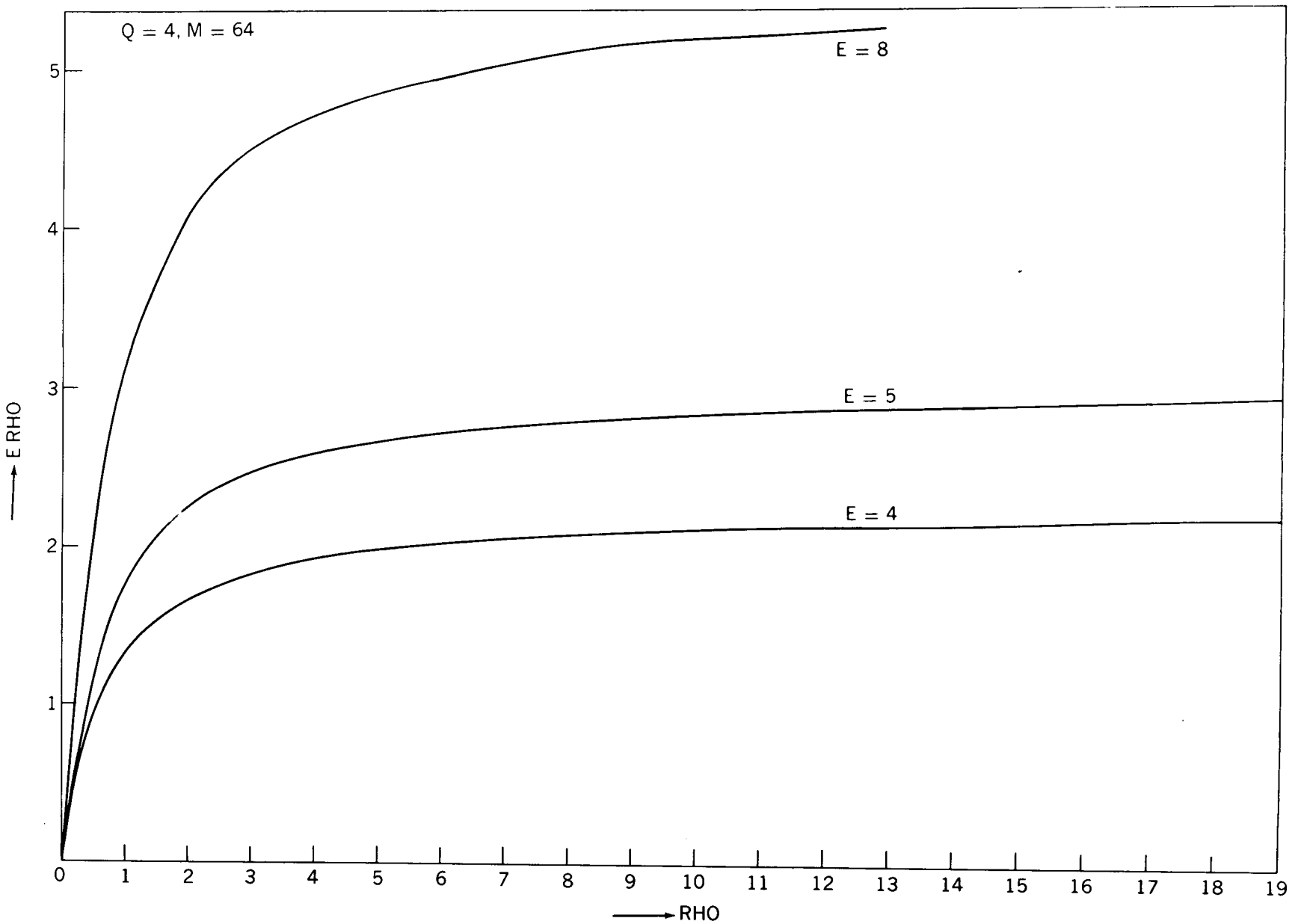

FIGURE 18

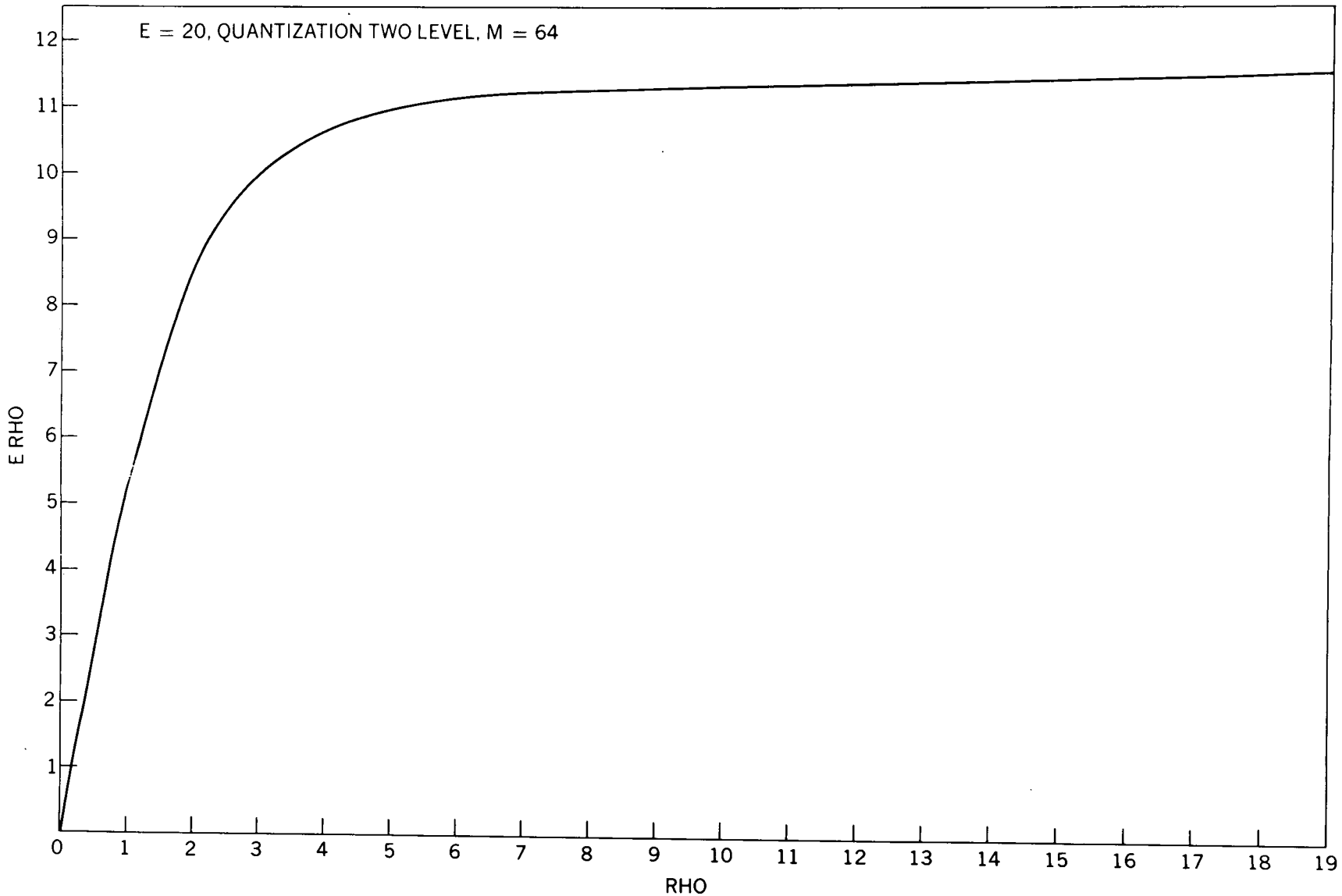
E = 20, QUANTIZATION TWO LEVEL, M = 64
E RHO
RHO
0
1
2
3
4
5
6
7
8
9
10
11
12
13
14
15
16
17
18
19

FIGURE 19

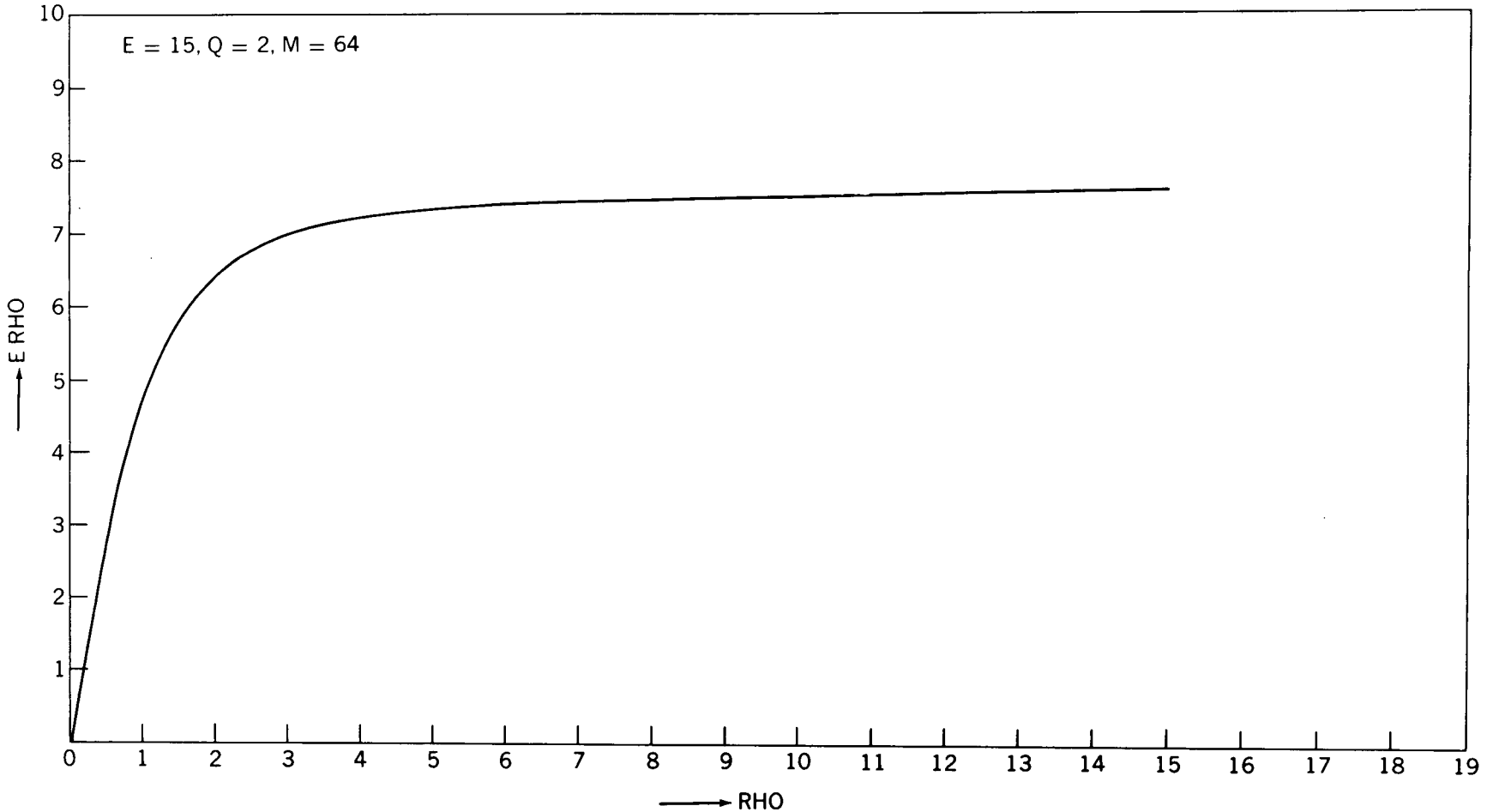

FIGURE 20

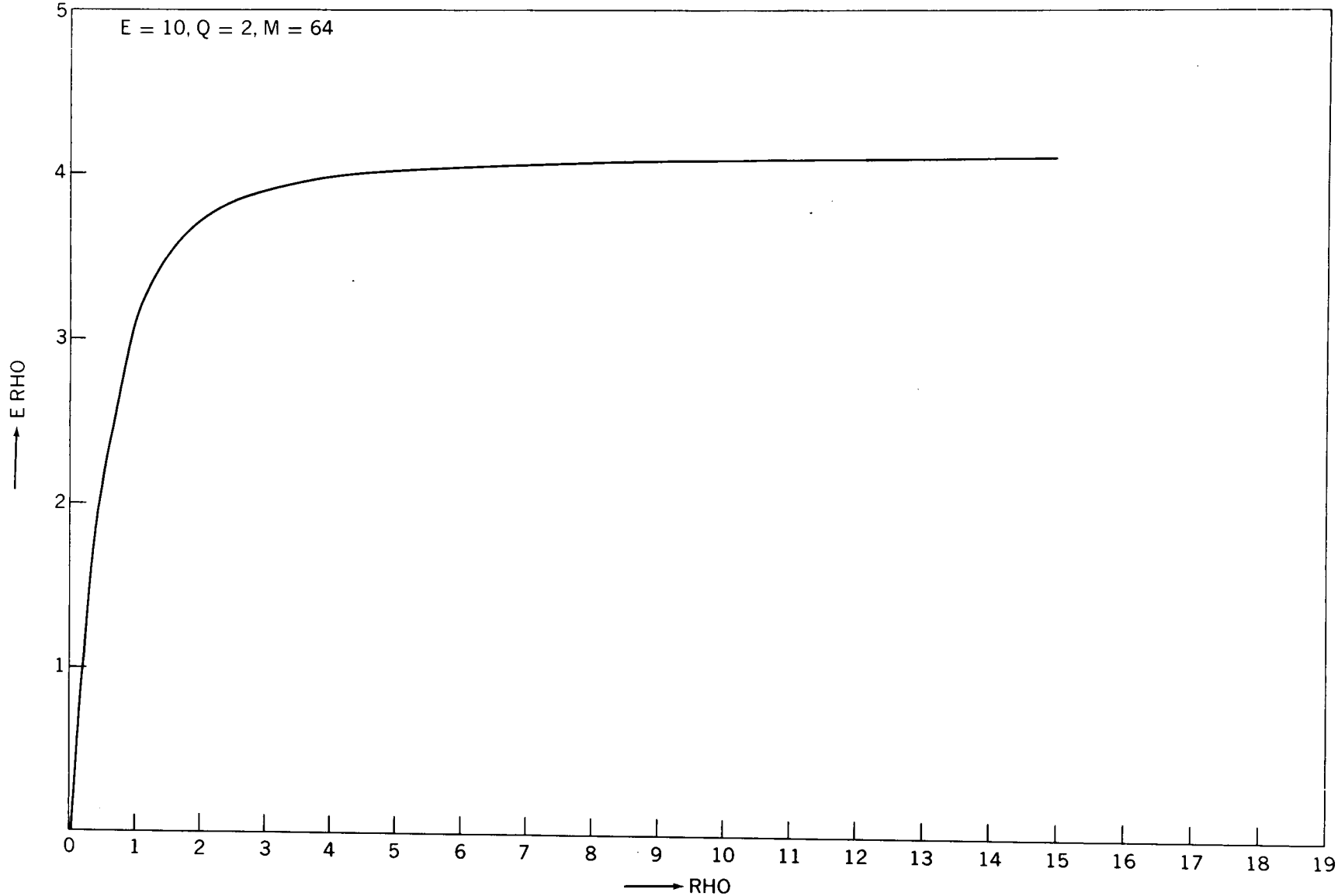

FIGURE 21

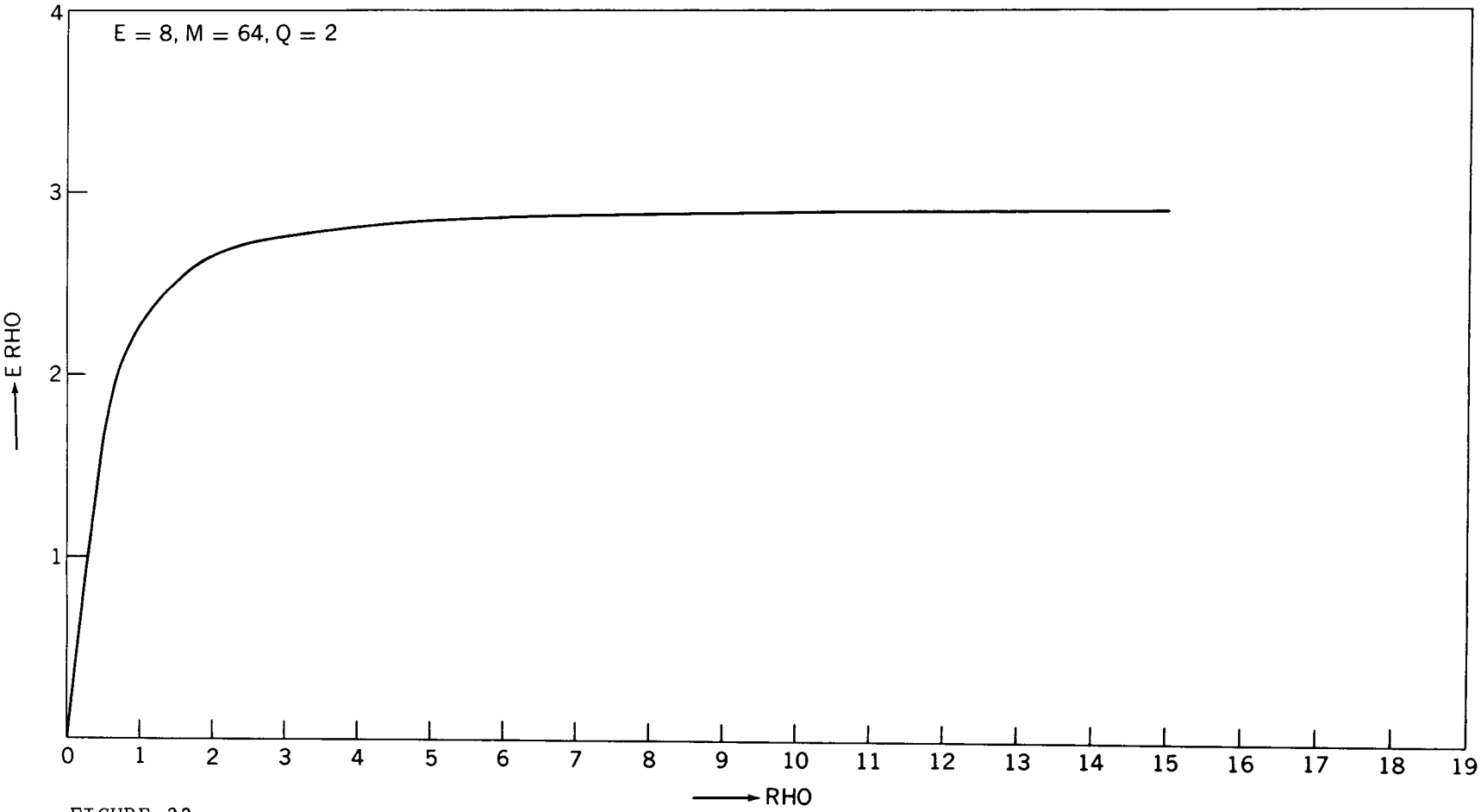

FIGURE 22

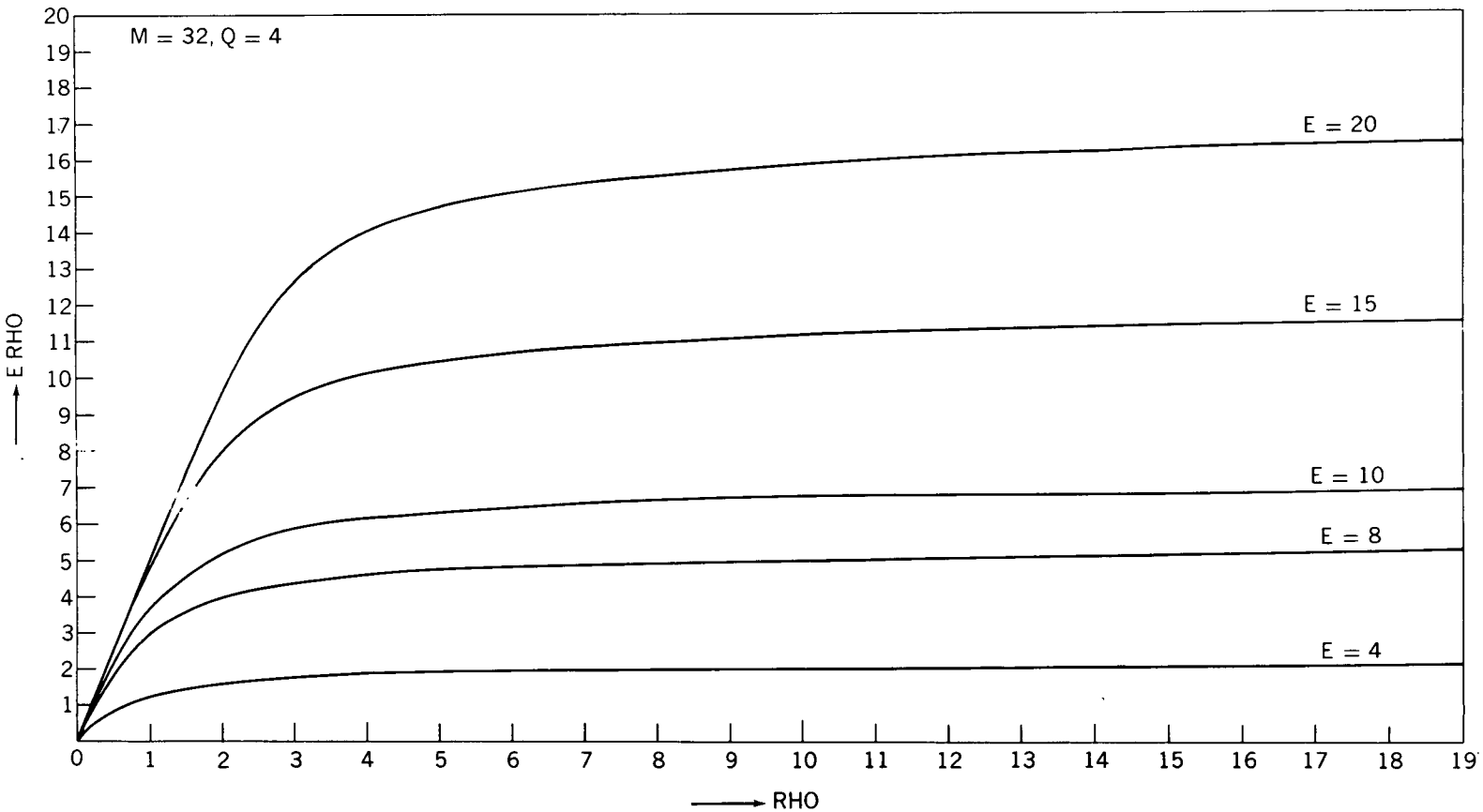
M = 32, Q = 4
E = 20
E = 15
E = 10
E = 8
E = 4
E RHO
RHO
0
1
2
3
4
5
6
7
8
9
10
11
12
13
14
15
16
17
18
19
20

FIGURE 23